SOURCE AND ENVIRONMENTAL PARAMETER ESTIMATION USING ELECTROMAGNETIC MATCHED FIELD PROCESSING

Peter Gerstoft[1] *and Donald F. Gingras*[2]

[1] Marine Physical Laboratory, University of California, San Diego, CA-92093-0701 USA

[2] Communication and Information Systems Department, SPAWAR, San Diego, CA 92152-7385 USA

ABSTRACT

Modern signal and array processing methods now incorporate the physics of wave propagation as an integral part of the processing. Matched field processing (MFP) refers to signal and array processing techniques in which, rather than a plane wave arrival model, complex-valued (amplitude and phase) field predictions for propagating signals are used. Matched field processing has been successfully applied in ocean acoustics and electromagnetics. In this paper, source localization performance via MFP is examined in the electromagnetics domain. Specifically, the impact of uncertainty in the *a priori* knowledge of the underlying physical parameters, atmospheric refractivity vs height, on source localization performance is examined.

1. INTRODUCTION

Recently research on electromagnetic array processing has included efforts to use precise full wave propagation models and efficient parameter search algorithms in order to estimate signal source location and environmental parameters [1]. MFP is a generalization of plane wave beamforming wherein the "steering or replica" vector is derived from a solution of the wave equation for a point source. Because the plane wave model is not generally an appropriate model for signals propagating in a waveguide MFP, provides improved estimation performance for this application.

In electromagnetics, the waveguide is strongly influenced by atmospheric phenomena. Two important atmospheric features found in the coastal region are the surface-layer evaporation duct and the elevated refractive layers at the top of the marine boundary layer. Both are caused by vertical gradients of temperature (increase) and humidity (decrease). The evaporation duct is surface-based and is persistent over ocean areas because of the rapid decrease of moisture immediately above the surface. Figure 1(a) illustrates a typical modified refractivity profile for the evaporation duct case. Elevated ducts occur when a stable atmospheric condition results in a temperature inversion and a sufficient amount of water vapor is trapped below that inversion. This condition causes a rapid decrease in the refractive index with increasing height leading to waveguide-like trapping. Figures 1(b) and (c) illustrate typical modified refractivity profiles for the surface-based and elevated duct cases.

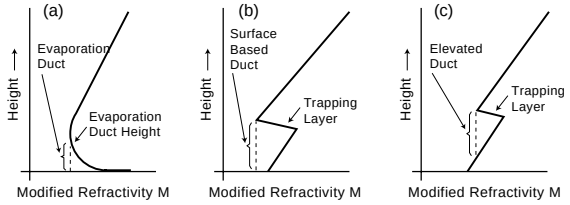

Figure 1: Modified refractivity M versus height. (a) Evaporation duct. (b) Surface-based duct. (c) Elevated duct.

A radio propagation experiment, Variability of Coastal Atmospheric Refractivity (VOCAR), was conducted during the summer of 1993 in the southern California bight. During this experiment three continuous wave transmissions at 144, 263 and 375 MHz were produced by transmitters on San Clemente Island. During a two week period radiosondes were launched at the midpoint of the over ocean path, a time series of refractivity profiles were calculated. This sequence of profiles is included as Fig. 2, it clearly illustrates the high degree of variability of refractivity profiles as a function of time. The impact of this variability of refractivity over time on the received signal level was reported in [2].

Precise knowledge of atmospheric refractivity allows one to predict the variability of received radio signal levels in the troposphere. In general, it is difficult to know the refractivity structure as a function of time and space. Recently, MFP methods were shown to be effective for estimating refractivity structure for known source location [3]. It was shown that a tri-linear approximation of the refractivity profile can be used in most cases. In this paper, the opposite problem is examined, that is, estimating the source location parameters when the refractivity structure is known or partially known. How well the refractivity structure must be known to accurately estimate source location parameters is the objective of this paper.

[0]This work was supported by the Office of Naval Research

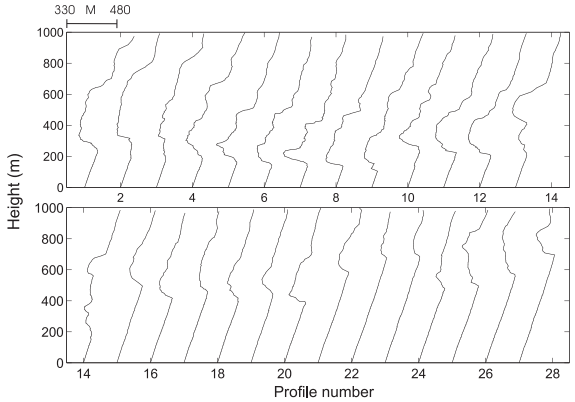

Figure 2: Time series of modified refractivity profiles taken during the VOCAR experiment period.

2. MFP OBJECTIVE FUNCTION

The objective function provides a measure of similarity between the observed signal field and the predicted signal field, where the observed signal field is the vector-valued array data and the predictions are based on the forward propagation model and environmental parameters. The linear Bartlett processor is perhaps the most popular. This processor expresses the linear correlation of the observed and computed field.

The Bartlett MFP objective function is generated as follows: Windowed time-series from an array are Fourier transformed to form frequency domain data vectors $\mathbf{d}^l(\omega_k)$ where ω_k denotes the k^{th} frequency and l the l^{th} time window. The dimension of the data vectors equals the number of antenna elements. The outer-products of the data vectors are averaged to form the sample covariance matrix

$$\hat{\mathbf{R}}(\omega_k) = (1/L)\sum_{l=1}^{L} \mathbf{d}^l(\omega_k)\mathbf{d}^l(\omega_k)^* \qquad (1)$$

where * denotes conjugate transpose and L is the number of time "snapshots." The normalized Bartlett objective function is then

$$P_{BT}(\mathbf{m};\omega_k) = \frac{\mathbf{w}^*(\mathbf{m})\hat{\mathbf{R}}(\omega_k)\mathbf{w}(\mathbf{m})}{\|\mathbf{w}(\mathbf{m})\|^2} \qquad (2)$$

where $\mathbf{w}(\mathbf{m})$ (referred to as the replica vector) is the vector of signal field predictions computed using a forward propagation model based on the parameter vector $\mathbf{m}$. In those cases where data are available at more than one frequency it is preferable to use a generalized objective by summing over multiple frequencies, $\omega_k; k = 1, \ldots, K$.

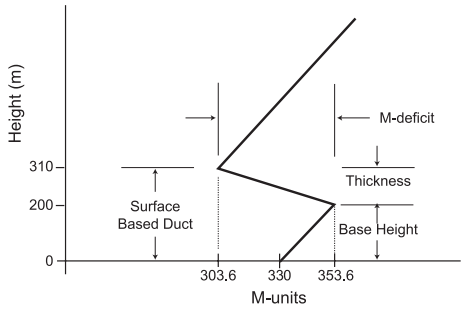

Figure 3: The tri-linear refractivity profile used in the simulations.

3. SIMULATION RESULTS

This section presents a discussion of the computer simulations for EM-MFP source localization in a tropospheric setting. In all simulations, the synthetic array data were generated for a scenario with the following general characteristics: Source Signal: The synthetic signal simulated an omni-directional point source with horizontal polarization at the three VOCAR frequencies, 143, 263, and 375 MHz. Source range was 60 km and source height was 18.6 m. Receive Antenna: The receive antenna was a vertical array containing 50 omnidirectional elements with an element spacing of 1 m, providing a total aperture of 49 m. Propagation Environment: The refractivity profile, in modified M-units, used was that of a surface based duct caused by an elevated trapping layer. Figure 3 illustrates the tri-linear profile used. This profile is the estimated tri-linear profile obtained in [3] for the twelfth profile of Fig. 2. The tri-linear profile is represented by three parameters: layer base height, layer thickness and layer M-deficit (decrease in refractivity over the layer in M-units). Propagation Code: The Terrain Parabolic Equation Model (TPEM) was used for all simulations [4]. TPEM is based on the split-step Fourier transform to solve the parabolic wave equation, and has been shown to be efficient. Objective Function: In all cases the objective function used was the Bartlett processor, Eq. 2. The synthetic signal data at each receive antenna element was generated using TPEM based on the source signal, receive element location, and propagation environment. The replica vectors were also generated using the TPEM propagation model.

Figure 4 illustrates the predicted propagation loss as a function of range and height at the three VOCAR frequencies for an emitter at 18.6 m. The tri-linear refractivity profile used is that of Fig. 3. The structure of the propagation loss as a function of range and height is quite similar for the three frequencies. Note the beam of energy that is refracted back to the surface by the trapping layer.

The source location estimates were obtained using range-height ambiguity surfaces. These surfaces were obtained by

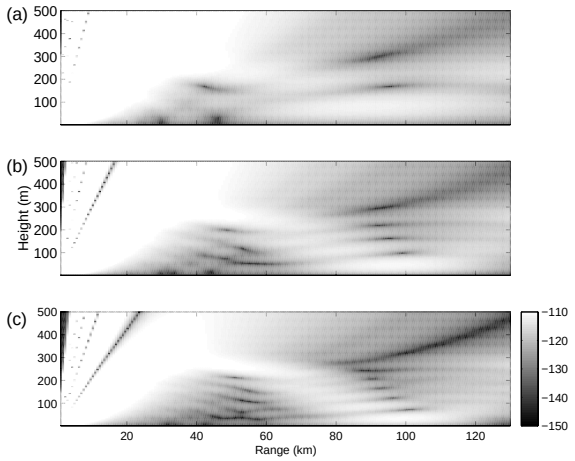

Figure 4: Coverage diagram for a source at 18.6 m at three frequencies: (a) 143 MHz, (b) 263 MHz and (c)375 MHz.

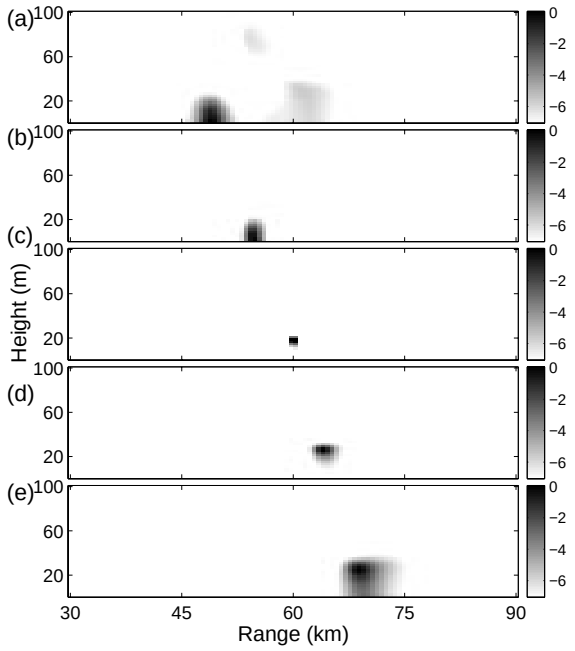

Figure 5: Range-height ambiguity surfaces for uncertainty in the layer base height value. The source was at 60 km range and 18.6 m height; the true layer base height was 200 m. Layer base height values are: (a) 160 m (b) 180 m (c) 200 m (d) 220 m (e) 240 m.

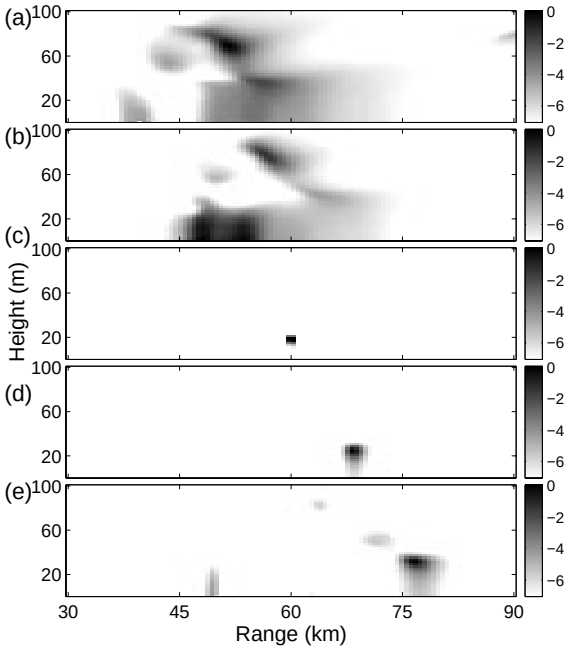

Figure 6: Range-height ambiguity surfaces for uncertainty in the layer thickness value. The source was at 60 km range and 18.6 m height; the true layer thickness was 110 m. Layer thickness values are: (a) 70 m (b) 90 m (c) 110 m (d) 130 m (e) 150 m.

plotting the value of the Bartlett objective function over a range interval of 0 to 90 km and a height interval of 0 to 100 m. The ambiguity surface maximum is one (or zero dB); a dynamic range of 6 dB is plotted. Three cases were examined: uncertainty in the layer base height, uncertainty in the layer thickness and uncertainty in the layer M-deficit.

Figure 5 illustrates the first result which indicates the effect of layer base height uncertainty on MFP source localization performance. As a reference point Fig. 5 (c) illustrates the case where all three tri-linear parameters are perfectly known. The other panels (a), (b), (d) and (e) illustrate the effect of using an incorrect value for the layer base height. When the base height was less that the actual base height, e.g., 160 m in panel (a) vice the true value of 200 m, the surface maxima, which indicate source localization estimates, are in error. Similar errors are seen for the other base height values. When the assumed base height value was less than the true value the source range and height were underestimated, and correspondingly, when the assumed base height value was greater than the true value the range and height were overestimated. It can be seen that the uncertainty in the layer base height value also causes the surface maxima to be less well defined.

Figure 6 illustrates the effect of layer thickness uncertainty on MFP source localization performance. As above Fig. 6 (c) illustrates the case where all three tri-linear param-

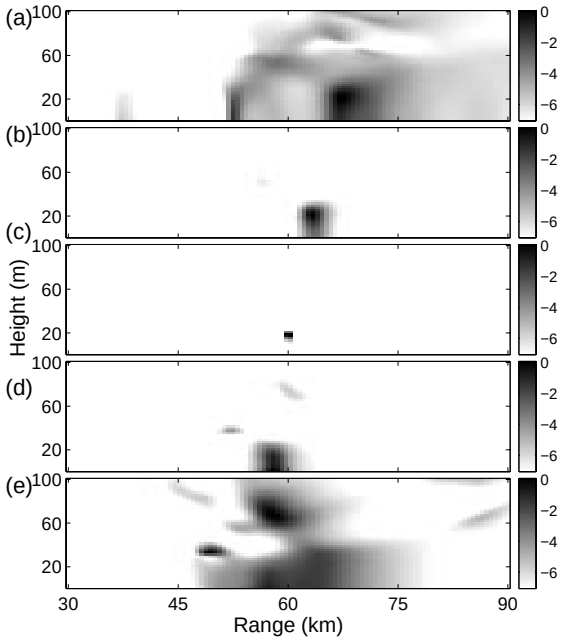

Figure 7: Range-height ambiguity surfaces for uncertainty in the layer M-deficit value. The source was at 60 km range and 18.6 m height; the true layer M-deficit was 110 M-units. Layer M-deficit values are: (a) 70 M-units (b) 90 M-units (c) 110 M-units (d) 130 M-units (e) 150 M-units.

eters are perfectly known. The other panels (a), (b), (d) and (e) illustrate the effect of using an incorrect value for the layer thickness. It is seen that the uncertainty in the layer thickness value had a fairly detrimental effect on the source location ambiguity surface. As above, the surface maxima, source range and height estimates, are incorrectly located and there is considerable sidelobe structure especially for thickness values that were less than the true value.

Figure 7 illustrates the effect of the layer M-deficit uncertainty on MFP source localization performance. Figure 7 (c) illustrates the case where all three tri-linear parameters are perfectly known. The other panels (a), (b), (d) and (e) illustrate the effect of using an incorrect value for the layer M-deficit. In this case the effect of the uncertainty is again fairly detrimental. The source location estimates are incorrect and there is considerable sidelobe structure.

Figure 8 illustrates the *a posteriori* distributions for the five estimated parameters using an antenna aperture of 50 m. The distributions were obtained using Genetic algorithms based estimation methods [1, 5]. The source location distributions are well defined compact distributions with maxima located close to the actual source location values. The distributions for the three tri-linear profile parameters are well defined. The overestimation of base height is compensated with an increase in M-deficit and a decrease in thickness so that the refraction occurs at about the same height and thus produces the same complex field at the receiving array.

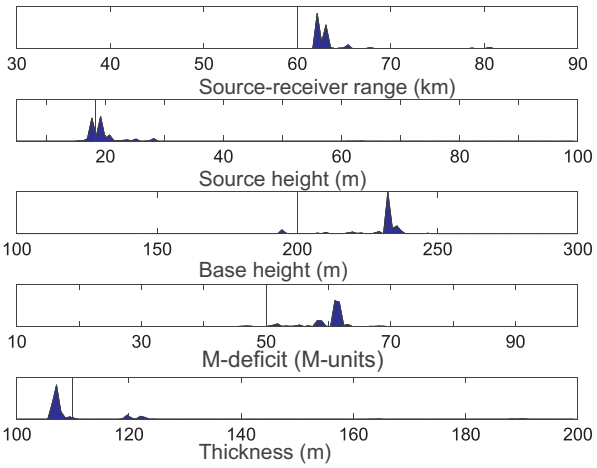

Figure 8: Genetic algorithm estimated *a posteriori* distributions for source range, source height, base height, M-deficit, and thickness. The solid line indicates the baseline values.

4. RESULTS AND CONCLUSIONS

These simulation results show that electromagnetic matched field processing methods can be used for source localization; even in the presence of uncertainty about the refractivity profile. It was seen that when the uncertainty was on the order of 10 to 20 % the source location estimates were fairly good, but for uncertainty greater than that the estimates were degraded significantly. All three tri-linear profile parameters appeared to have equal effect on the source localization performance. Finally, when all five parameters were estimated, good source location estimates were obtained even though the tri-linear profile parameters were in error.

5. REFERENCES

[1] D.F. Gingras, P. Gerstoft and N.L. Gerr, "Electromagnetic matched field processing: Basic concepts and tropospheric simulations," *IEEE Trans. Antennas Propagat.*, vol. 42, pp. 1305–1316, Oct. 1997.

[2] L.T. Rogers, "Effects of the variability of atmospheric refractivity on propagation estimates," *IEEE Trans. Antennas Propagat.*, vol. 44, pp. 460–465, Apr. 1996.

[3] P. Gerstoft, D.F. Gingras, L.T. Rogers and W.S. Hodgkiss, "Estimation of radio refractivity structure using matched field array processing," submitted to *IEEE Trans. Antennas Propagat.*, 1998.

[4] A.E. Barrios, "A terrain parabolic equation model for propagation in the troposphere," *IEEE Trans. Antennas Propagat.*, vol. 42, pp. 90–98, Jan. 1994.

[5] P. Gerstoft, "Inversion of seismoacoustic data using genetic algorithms and *a posteriori* probability distributions," *J. Acoust. Soc. Am.*, vol. 95, pp. 770–782, Feb. 1994.